Structural Volume Changes upon Photoexcitation of Porphyrins: Role of the Nitrogen−Water Interactions

Thomas Gensch,[†] Cristiano Viappiani,[‡] and Silvia E. Braslavsky*,[†]

Contribution from the Max-Planck-Institut für Strahlenchemie, Postfach 101365, D-45413 Mülheim an der Ruhr, Germany, and Dipartimento di Fisica, Università di Parma and Istituto Nazionale per la Fisica della Materia (INFM), viale delle Scienze, 43100 Parma, Italia

Received April 27, 1999. Revised Manuscript Received August 23, 1999

Abstract: The molecular structural volume change (as determined by laser-induced optoacoustics), $\Delta V_R \sim -18$ Å^3, accompanying triplet state formation of free base 5,10,15,20-tetrakis-(4-sulfonatophenyl)-porphine ($TSPP^{4-}$) in aqueous solutions of pH > 5.5, was markedly decreased to -5 Å^3 for the dimer, to -3.5 Å^3 for $ZnTSPP^{2-}$, and to -4 Å^3 for the nonionic micelle-included free base tetraphenyl porphyrin. For the free bases of other meso-substituted porphyrins with cationic side-groups such as 5,10,15,20-tetrakis-(4-methylaminophenyl)-porphine ($TMAPP^{4+}$) and 5,10,15,20-tetrakis-(4-methylpyridyl)-porphine, similar large contractions as for monomeric $TSPP^{4-}$ were determined upon triplet formation, that decreased also on lowering pH to ~ -5 Å^3 for H_2TSPP^{2-} (pH 4) and to ~ -4 Å^3 for H_2TMAPP^{6+} (pH 2.2). The triplet state quantum yield was not markedly affected by pH changes, oligomerization (mostly as a dimer), or complexation. The value of $pK_a = 5.1-5.2$ derived from the titration of ΔV_R for formation (and decay) of triplet $TSPP^{4-}$ is identical to that for the equilibrium of free base and monoprotonated forms, derived from fittings of the pH-dependent absorption and fluorescence data. For $TMAPP^{4+}$ the $pK_a = 3.5$ from titration of the contraction (triplet formation) coincided with that for the transition mono-/diprotonated species, whereas upon triplet decay the expansion showed a $pK_a = 4.0$ similar to the value for monoprotonated/free-base equilibrium. The contraction upon triplet formation in the free base porphyrins mainly originates in the rearrangement of water around the excited macrocycle nitrogen atoms and to a minor extent in a contraction due to bonds shortening upon excitation. The contribution of the chromophore-solvent interactions is thus reduced upon impairment of hydrogen bridges between the nitrogen lone electron pairs and water by dimer formation, metal complexation, and protonation.

Introduction

Time-resolved laser-induced optoacoustic spectroscopy (LIOAS) measurements at various temperatures have been used to investigate the structural volume changes accompanying light-induced photochemical processes in aqueous solutions.[1−4] Photoinduced volume changes originate in thermal deactivation of the excited states (ΔV_{th}) and in molecular structural changes (ΔV_r).[2−5] The thermal contribution ΔV_{th} depends on the temperature through the ratio of thermoelastic parameters ($\beta/c_p\rho$), which is strongly temperature dependent for aqueous solutions due to the important variation of the thermal expansion coefficient β in these solutions. Therefore, measurements in a relatively narrow temperature range allow the separation of ΔV_{th} and ΔV_r.[2,3,5−8]

The use of deconvolution of photoacoustic waveforms has increased time resolution, permitting the detection of the photoinduced structural changes in a time range between ~5 ns and about 10 μs.[1,9−17] We have recently used a two temperature (TT) method, in conjunction with deconvolution, as an alternative to the several-temperature (ST) method for the determination of the laser-induced structural volume changes.[1,15]

Some evidence has been accumulated in the past few years about the molecular origin of the structural volume changes. The structural volume change concomitant with the photoisomerization of cyanines was attributed to changes in the specific interactions with the solvent molecules (a mixture of

* Address correspondence to this author. Fax: +49 (208) 306-3951. E-mail: braslavskys@mpi-muelheim.mpg.de.

[†] Max-Planck-Institut für Strahlenchemie

[‡] Università di Parma and Istituto Nazionale per la Fisica della Materia

(1) Gensch, T.; Braslavsky, S. E. *J. Phys. Chem.* **1997**, *101*, 101.

(2) Braslavsky, S. E.; Heibel, G. E. *Chem. Rev.* **1992**, *92*, 1381.

(3) Peters, K. S.; Snyder, G. J. *Science* **1988**, *241*, 1053.

(4) Schulenberg, P. J.; Braslavsky, S. E. In *Progress in Photothermal and Photoacoustic Science and Technology*; Mandelis, A., Hess, P., Eds.; Life and Earth Sciences. SPIE Press: New York, 1997; Vol. 3, pp 58−81.

(5) Callis, J. B.; Parson, W. W.; Gouterman, M. *Biochim. Biophys. Acta* **1972**, *267*, 348.

(6) Goodman, J. L.; Herman, M. S. *Chem. Phys. Lett.* **1989**, *163*, 417.

(7) Yruela, I.; Churio, M. S.; Gensch, T.; Braslavsky, S. E.; Holzwarth, A. R. *J. Phys. Chem.* **1994**, *98*, 12789.

(8) Malkin, S.; Churio, M. S.; Shochat, S.; Braslavsky, S. E. *J. Photochem. Photobiol. B: Biol.* **1994**, *23*, 79.

(9) Small, J. R. In *Numerical computer methods*; Brand, L.; Johnson, M. L., Eds.; Academic Press: San Diego, 1992; Vol. 210, pp 505−521.

(10) Rudzki, J. E.; Goodman, J. L.; Peters, K. S. *J. Am. Chem. Soc.* **1985**, *107*, 7849.

(11) Small, J. R.; Kurian, E. *Spectroscopy* **1995**, *10*, 27.

(12) Habib Jiwan, J.-L.; Wegewijs, B.; Indelli, M. T.; Scandola, F.; Braslavsky, S. E. *Recl. Trav. Chim. Pays-Bas* **1995**, *114*, 542.

(13) Peters, K. S.; Watson, T.; Marr, K. *Annu. Rev. Biophys. Biophys. Chem.* **1991**, *20*, 343.

(14) Norris, C. L.; Peters, K. S. *Biophys. J.* **1993**, *65*, 1660.

(15) (a) Bonetti, G.; Vecli, A.; Viappiani, C. *Chem. Phys. Lett.* **1997**, *269*, 268. (b) Viappiani, C.; Abbruzzetti, S.; Small, J. R.; Libertini, L. J.; Small, E. W. *Biophys. Chem.* **1998**, *73*, 13. (c) Losi, A.; Viappiani, C. *Chem. Phys. Lett.* **1998**, *289*, 500.

(16) Schmidt, R.; Schütz, M. *J. Photochem. Photobiol. A: Chem.* **1996**, *103*, 39.

(17) Zhang, D.; Mauzerall, D. C. *Biophys. J.* **1996**, *71*, 381.

10.1021/ja9913885 CCC: $18.00
Published on Web 10/30/1999

water/ethanol) between the parent compound and the photoisomer, with a dipole moment different from that of the parent molecule.[18]

Electrostriction[19,20] has been claimed to be the origin of the structural volume changes observed in intermolecular electron-transfer reactions[21,22] and upon photoexcitation of photosynthetic reaction centers.[23] We have also invoked electrostriction in order to explain the values of the structural volume change found upon photoinduced intramolecular electron transfer in nonpolar organic solvents.[24,25]

However, results obtained in our laboratories show that the electrostrictive contribution is by far not enough to account for the observed structural volume changes in aqueous solution, neither in intramolecular[12,26,27] nor in intermolecular electron-transfer reactions,[28,29] proton-transfer reactions,[15] or photoisomerizations,[18] when the molecules reacting strongly interact with water by means of hydrogen bridges. In some cases it was possible to obtain a relatively good agreement between the experimental value for the structural volume change and the one calculated by using the equation for electrostriction with a semiempirical constant instead of the theoretical one. This was the case, for example, for the photoinduced proton production.[30]

For photoinduced electron-transfer reactions with compounds forming hydrogen bridges, the magnitude of the structural volume change, as well as that of the heat evolved, is determined mainly by the organization of the water structure around the chromophore.[12,26,27] This structure may be perturbed by the addition of different salts.[26] Very recently, we demonstrated the same effect for a photoinduced intermolecular electron-transfer reaction between the triplet metal-to-ligand charge transfer state of $Ru(bpy)_3^{2+}$ as electron donor and the methyl viologen dication as acceptor, again in aqueous solutions with various added salts.[31]

The production of porphyrin triplet states is also in some cases accompanied by structural volume changes.[1,7,21] In particular, we have shown that the formation of the triplet state of the free base 5,10,15,20-tetrakis-(4-sulfonatophenyl)-porphine ($TSPP^{4-}$) in aqueous solutions at pH > 7 is accompanied by a contraction of -18 Å^3 (± 5 Å^3), followed by an expansion of the same magnitude upon triplet decay.[1] We tentatively assigned the structural volume changes to changes in the solvation sphere of the porphyrin upon formation (and decay) of the excited state. In view of the time resolution of the LIOAS experiments we could not discriminate whether the contraction occurred already upon formation of the singlet state. The expansion concomitant with the triplet decay was independent of the interaction with molecular oxygen.

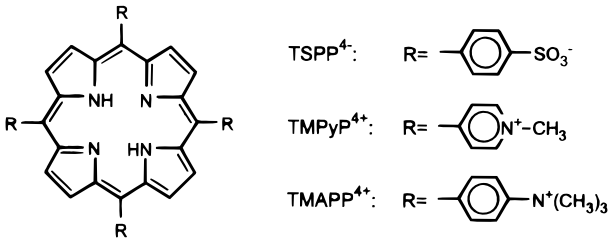

Figure 1. Chemical structures of the porphyrins used in this study. Protonation changes in the pH range 3−8 occur at the central nitrogens.

In this paper we further examine the structural volume changes photoinduced in $TSPP^{4-}$ aqueous solutions by considering the effect on ground and excited-state properties of oligomerization, metal complexation, and pH, in view of the fact that all of these reactions involve the lone electron pairs on the central nitrogen atoms in the macrocycle. Additionally, the possible effect of the 4-sulfonatophenyl group on the observed volume changes is investigated by studying several free-base porphyrins with other substituents at the meso-position of the porphyrin macrocycle.

Experimental Section

Chemicals. 5,10,15,20-tetrakis-(phenyl)-porphine, 5,10,15,20-tetrakis-(4-sulfonatophenyl)-porphine dihydrochloride, the Zn-5,10,15,20-tetrakis-(4-sulfonatophenyl)-porphine dihydrochloride; 5,10,15,20-tetrakis-(*N*-methyl-4-pyridyl)-porphine-tetra-(toluol-4-sulfonate) (see Figure 1 for abbreviations) were purchased from Porphyrin Products (Logan, Utah). Evans blue (EB) and 2-hydroxybenzophenone (HBP) were from Aldrich (Deisenhofer). 5,10,15,20-tetrakis-(4-methyl-aminophenyl)-porphine-tetra-(toluol-4-sulfonate) (see Figure 1 for abbreviation), bromocresol purple (5,5′-dibromo-*o*-cresol-sulfonaphthaleine, BCP), rose bengal (4,5,6,7-tetrachloro-2′,4′,5′,7′-tetraiodo-fluorescein), Triton X-100, and D_2O were from Fluka (Buchs, Switzerland).

Solutions. Experiments were carried out either in air-saturated 100 mM Na acetate buffer, or in 10 mM Tris-buffer with various amounts of NaCl (0 to 1 M). All experiments were at room temperature (22 ± 2) °C unless otherwise stated. For LIOAS and excitation at 355 and 308 nm the concentration of the porphyrins was between 2 and 4 μM. When exciting at 532 nm the concentration was ~20 μM. For the emission experiments the concentration was ~5 μM. For the titrations, 0.1−2 M HCl solutions were used.

TPP was dissolved in 10 mM Triton X-100 (the critical micelle concentration for this surfactant at 25 °C is 0.26×10^{-3} M)[32] to obtain an absorbance of 0.2 at the excitation wavelength (532 nm).

For the time-resolved measurement of the near-infrared phosphorescence emission of singlet molecular oxygen, $O_2(^1\Delta_g)$, the various porphyrins were dissolved in the respective buffers and micellar solutions with D_2O instead of H_2O.

Absorption spectra were taken using a UV-2102 spectrophotometer (Shimadzu).

Emission Data. Steady-state fluorescence spectra were recorded with a Spex Fluorolog equipment as described previously.[33] Time-resolved fluorescence was measured with a home-built single-photon counting apparatus based on a photomultiplier with enhanced red sensitivity.[34] It allows measurements of fluorescence lifetimes between 100 ps and 100 ns. The time-resolved phosphorescence detection (TRPD) of the $O_2(^1\Delta_g)$ near-infrared emission ($\lambda_{max} = 1270$ nm) was performed with

(18) Churio, M. S.; Angermund, K. P.; Braslavsky, S. E. *J. Phys. Chem.* **1994**, *98*, 1776.
(19) Drude, P.; Nernst, W. *Z. Phys. Chem. (Leipzig)* **1894**, *15*, 79.
(20) le Noble, W. J.; Kelm, H. *Angew. Chem.* **1980**, *19*, 841.
(21) Feitelson, J.; Mauzerall, D. C. *J. Phys. Chem.* **1996**, *100*, 7698.
(22) Feitelson, J.; Mauzerall, D. C. *J. Phys. Chem.* **1993**, *92*, 8410.
(23) Mauzerall, D. C.; Gunner, M. R.; Zhang, J. W. *Biophys. J.* **1995**, *68*, 275.
(24) Wegewijs, B.; Verhoeven, J. W.; Braslavsky, S. E. *J. Phys. Chem.* **1996**, *100*, 8890.
(25) Wegewijs, B.; Paddon-Row: M. N.; Braslavsky, S. E. *J. Phys. Chem. A* **1998**, *102*, 8812.
(26) Borsarelli, C. D.; Braslavsky, S. E. *J. Phys. Chem. B* **1998**, *102*, 6231.
(27) Borsarelli, C. D.; Braslavsky, S. E. *J. Phys. Chem. B* **1997**, *101*, 6036.
(28) Habib Jiwan, J.-L.; Chibisov, A.; Braslavsky, S. E. *J. Phys. Chem.* **1995**, *99*, 10246.
(29) Borsarelli, C. D.; Corti, H.; Goldfarb, D.; Braslavsky, S. E. *J. Phys. Chem. A* **1997**, *101*, 7718.
(30) Borsarelli, C. D.; Braslavsky, S. E. *J. Photochem. Photobiol. B: Biol.* **1998**, *43*, 222.
(31) Borsarelli, C. D.; Braslavsky, S. E. *J. Phys. Chem. B* **1999**, *103*, 1719.
(32) Fendler, J. H. *Membrane Mimitic Chemistry*; Wiley: New York, 1982; p 9.
(33) Holzwarth, A. R.; Lehner, H.; Braslavsky, S. E.; Schaffner, K. *Liebigs Ann. Chem.* **1978**, 2002.
(34) Hildenbrand, K.; Nicolau, C. *Biochim. Biophys. Acta* **1979**, *553*, 365.

a liquid nitrogen cooled germanium detector (EO817FP, NorthCoast, rise time 200 ns) as described earlier.[7,35] Rose bengal [$O_2(1\Delta_g)$ quantum yield, $\Phi_\Delta = 0.76$][36] and $TSPP^{4-}$ ($\Phi_\Delta = 0.60$)[1,37] were used as reference compounds.

Laser Flash Photolysis. Laser flash photolysis with absorption detection (LFP) was performed with a home-built flash photolysis equipment using a Nd:YAG-pumped dye-laser (JK Lasers, Rugby, UK, 11 ns pulses) with excitation wavelengths between 568 and 650 nm.[38]

LIOAS. The setup for the LIOAS experiments has been described in several of our publications.[1,7,8,12,26−30] The second (532 nm) or the third harmonic (355 nm) of a Q-switched Nd:YAG laser (Spectron Lasers, Rugby, UK, 8 ns pulses) or a Nd:YAG-2nd harmonic-pumped dye laser (635, 651 nm; Spectron Lasers) were used as excitation sources. The beam was shaped by a slit (0.5 to 1.0 mm width) in front of the cuvette. All experiments were performed with low photon fluxes providing at most excitation of 15% of the sample molecules within the excited volume. In some cases, excitation was with the 308 nm beam from a XeCl excimer laser (EMG 50, Lambda Physik, Göttingen, Germany, 8 ns pulses).

The LIOAS signal handling has been extensively described in the past.[3,9,10,12,39] The calorimetric references providing the instrumental function to be used in deconvolution were EB and BCP.[8]

The ratio of thermoelastic parameters of the various aqueous solutions was determined for the temperature range 5−12 °C, by a comparative method using BCP as a reference compound in the buffered solution and EB in neat water. The data for the buffer were thus obtained using the equations already presented and the literature values for water.[18] $T_{\beta=0}$ was determined with an accuracy of 0.1 °C by searching for the disappearance of the reference signal in the different buffer systems, and resulted to be 2.7 °C for 10 mM Tris buffer, 2.9 °C for 100 mM Na acetate buffer, and 1, 0.5, −0.5, and −2.5 °C for 10 mM Tris buffer with 100, 140, 310 mM, and 1 M NaCl, respectively.

The structural volume changes were determined by using a two-temperature (TT) method.[1] The reference waveform was acquired at the temperature $T_{\beta\neq0}$ (6, 8, 10, or 12 °C), whereas the sample signal was acquired at $T_{\beta\neq0}$ and at the temperature $T_{\beta=0}$ at which the value of β, the thermal expansion coefficient of the solution, vanishes. The molar structural volume change $\Delta V_{R,i}$ was readily obtained from the amplitudes φ_i of the LIOAS signals biexponential fitting by using eq 1, in which $i = 1$ corresponds to the prompt signal and $i = 2$ corresponds to the delayed signal.[1]

$$\Phi_T \Delta V_{R,i} = \varphi_i E_\lambda \left(\frac{\beta}{c_p \rho}\right)_{T_{\beta\neq0}} \quad (1)$$

An advantage of measuring the sample at $T_{\beta=0}$ arises from the negligible volume difference of $O_2(^1\Delta_g)$, as compared to ground-state molecular oxygen, $O_2(^3\Sigma_g)$, (<0.2 Å^3).[1,21] Inasmuch as there is no contribution from $O_2(^1\Delta_g)$ at $T_{\beta=0}$, $O_2(^1\Delta_g)$ decay should not interfere with the porphyrin triplet decay which constituted a problem for the deconvolution analysis at $T_{\beta\neq0}$.[1]

To measure the water-insoluble porphyrin TPP in the micelles, it was necessary to check whether the TT method was still applicable in this two-phase system. Since TPP dissolves in the organic phase, the hydrophobic HBP was chosen as a calorimetric reference for the TT measurements. $T_{\beta=0}$ of the nonionic micellar dispersion (10 mM Triton X-100) was determined with BCP, which preferentially dissolves in the aqueous phase. Comparison of the signals from HBP and BCP at $T_{\beta=0}$ showed a small positive signal for HBP, probably due to an expansion of the micelles due to the heat release. This signal, however, was very small, and a 0.2 °C drop of the temperature led to its disappearance. Since the prompt heat release by the sample TPP was half of that by the reference, the expansion due to heat release by HBP is comparable to a mismatch in $T_{\beta=0}$ of 0.1 °C, which was the uncertainty of our temperature control. Thus, this small signal originating from expansion of the micellar phase at $T_{\beta=0}$ was ignored. The structural volume change signal of TPP at $T_{\beta=0}$ was at least 10 times larger, which is outside the experimental error.

Table 1. $O_2(^1\Delta_g)$ Quantum Yields, Φ_Δ, Obtained by TRPD upon Excitation of Air-Saturated Solutions of the Various Free-base Porphyrins, the Diprotonated Forms, $ZnTSPP^{2-}$, and the $TSPP^{4-}$ Dimer, $(TSPP^{4-})_2$

compound	pH	Φ_Δ (± 0.05)	literature Φ_Δ
$TSPP^{4-}$	7	0.62[a]	0.63,[37] 0.64,[41] 0.65[42]
H_2TSPP^{2-}	3.5	0.51[b]	
$(TSPP^{4-})_2$	7.8[c]	0.58[a]	0.51[37]
$TMPyP^{4+}$	7	0.58[b]	0.74,[36] 0.9[43e]
$TMAPP^{4+}$	7	0.56[b]	0.48−0.85[36,44]
H_2TMAPP^{6+}	2.2	0.55[b]	
$ZnTSPP^{2-}$	7	0.67[d]	0.77[36]
TPP in Triton-X micelles		0.58[a]	0.55

[a] $\lambda_{exc} = 532$. [b] $\lambda_{exc} = 355$. [c] With 430 mM NaCl. [d] $\lambda_{exc} = 568$. [e] Calculated using as a standard $\Phi_\Delta(TSPP^{4-}) = 0.7$ and with 10% error.[43]

The triplet lifetimes obtained by LFP are much more precise than those obtained by deconvolution of the LIOAS signals due to the strong correlation between the lifetimes and the amplitudes in the latter method. For the analysis of the LIOAS experiments we fixed in some cases the triplet lifetime to the values measured with LFP, in order to obtain during the deconvolution procedure more precise values for φ_1 and φ_2, to be then used in eq 1.

The triplet quantum yield, $\Phi_T = 0.61$, was measured directly by LIOAS for $TSPP^{4-}$[1] and a lower limit was estimated indirectly from the $O_2(^1\Delta_g)$ formation quantum yield, Φ_Δ, for the other porphyrins.

Results

Triplet States Properties of $TSPP^{4-}$. The triplet and $O_2(^1\Delta_g)$ lifetimes obtained by TRPD in deuterated buffers at 12 °C were in accordance with the expected values for the triplet-O_2 energy transfer rate and $O_2(^1\Delta_g)$ decay (the latter between 60 and 65 μs).[40] Φ_Δ values between 0.51 and 0.67 were obtained (Table 1). For $TSPP^{4-}$ the determined value of $\Phi_\Delta = 0.62 \pm 0.03$ (average of 5 independent measurements) is in reasonable agreement with the reported values 0.63,[37] 0.64,[41] and 0.65.[42] We consider these values more reliable than the previously reported numbers in the range 0.3−0.76.[36] We used $TSPP^{4-}$ as an internal standard for excitation at 355, 568, 635, and 651 nm.

The triplet lifetimes estimated from the rising part in the TRPD (0.8−3 μs) signal showed a large error. More accurate values were obtained by nanosecond LFP (Table 2).

Substitution Effects. The structural volume changes for the triplet formation in aqueous solutions of the free base forms of $TSPP^{4-}$, $TMPyP^{4+}$, and $TMAPP^{4+}$ were all similar (Table 2). Excitation was accompanied by a contraction of (−17.0 ± 1.5) Å^3 that reverted upon decay of the triplet state to the ground state.

Dimer of $TSPP^{4-}$. In view of the fact that the absorption spectrum of $TSPP^{4-}$ in solutions of pH > 5.5 changes upon either increasing the porphyrin concentration or adding salts, for example, NaCl,[45,46] experiments aiming at the selective excitation of the dimer were performed at high salt concentration. The excitation wavelength was also chosen such as to have

(35) Martínez, G.; Bertolotti, S. G.; Zimerman, O. E.; Mártire, D. O.; Braslavsky, S. E.; García, N. A. *J. Photochem. Photobiol. B: Biol.* **1993**, *17*, 247.
(36) Wilkinson, F.; Helman, W. P.; Ross, A. B. *J. Phys. Chem. Ref. Data* **1993**, *22*, 113.
(37) Tanielian, C.; Wolf, C.; Esch, M. *J. Phys. Chem.* **1996**, *100*, 6555.
(38) Schmidt, P.; Gensch, T.; Remberg, A.; Gärtner, W.; Braslavsky, S. E.; Schaffner, K. *Photochem. Photobiol.* **1998**, *68*, 754.
(39) Rothberg, L. J.; Simon, J. D.; Bernstein, M.; Peters, K. S. *J. Am. Chem. Soc.* **1983**, *105*, 3464.
(40) Wilkinson, F.; Helman, W. P.; Ross, A. B. *J. Phys. Chem. Ref. Data* **1995**, *24*, 663.
(41) Davila, J.; Harriman, A. *Photochem. Photobiol.* **1990**, *51*, 9.
(42) Krasnovsky, A. A., Jr. *SPIE Proc.* **1993**, *1887*, 177.

Table 2. Triplet Lifetimes, τ_T, and Structural Volume Changes for Its Formation, $\Delta V_{R,1}$, and Decay, $\Delta V_{R,2}$, in Air-Saturated Solutions as Determined by LFP and LIOAS

compound	pH	τ_T[a] (μs)	τ_T[b] (μs)	$\Phi_T\Delta V_{R,1}$ (Å^3)	$\Phi_T\Delta V_{R,2}$ (Å^3)	$\Delta V_{R,1}$[c] (Å^3)	$\Delta V_{R,2}$[c] (Å^3)
$TSPP^{4-}$	7	1.8	1.5−2.0	−11.3[d]	8.9	−18	14.5
H_2TSPP^{4-}	3.5	1.9	1.7−2.1	−2.9	2.3	−5	4
$(TSPP^{4-})_2$	7.8[e]	2.8	2.2−3.2	−3.0	2.6	−5	4.5
$TMPyP^{4+}$	7	2.0	1.9−2.6	−9.5	7.5	−16.5	13
$TMAPP^{4+}$	7	1.8	1.6−1.9	−10	9.3	−16	15
H_2TMAPP^{6+}	2.2	1.9	1.7−2.0	−2.3	2.8	−4	4.5
$ZnTSPP^{2-}$	7	2.85	1.3−3.7	−2.3	2.1	−3.5	3
TPP in Triton X-100 micelles		2.65	2.2−3.2	−2.3	2.0	−4	3.5

[a] From LFP, λ_{exc} = between 568 and 650 nm depending on the porphyrin. [b] From LIOAS. [c] With $\Phi_\Delta = \Phi_T$ in eq 1 and the values in Table 1, [d] Extrapolated from data in Figure 2. [e] In the presence of 430 mM NaCl.

maximal dimer excitation (651 nm affords 99% dimer excitation in NaCl 1M).

The fluorescence lifetime and quantum yield for the dimer, $\tau_F = 5.6$ ns and $\Phi_F = 0.04 \pm 0.01$ upon 355 nm excitation of a solution containing 0.43 M NaCl were smaller than the respective values for the monomer, $\tau_F = 9.6$ ns and $\Phi_F = 0.058$.[1] The emission spectrum of the dimer shows a red shift of 12 nm with a weaker shoulder in the red (data not shown) as already reported by Ravikant et al.[46]

The triplet lifetime of $TSPP^{4-}$ was markedly prolonged for the dimer (2.8 μs instead of 1.8 μs, Table 2) as monitored by triplet−triplet absorption at 460 nm in 10 mM Tris buffer at pH 7.8 after pulse excitation at 635 nm for the monomer and 568 nm for the dimer (1 M NaCl).

TRPD data show that Φ_Δ after excitation at 650 nm decreased by less than 20% for the dimer, suggesting that Φ_T is essentially unaffected by dimerization (see Table 1) as already reported.[37]

Deconvolution of the LIOAS waveform for a 20 μM solution of $TSPP^{4-}$ in 10 mM Tris buffer at pH 7.8 and $T_{\beta=0} = 2.7$ °C with that for the EB reference solution acquired at $T_{\beta\neq0}$ afforded a biexponential time evolution of ΔV_R, that is, a fast, subresolution relatively large contraction and an expansion with a lifetime of ~2 μs. The structural volume changes have been attributed to the formation ($\Delta V_{R,1}$) and the decay ($\Delta V_{R,2}$) of the triplet state of $TSPP^{4-}$.[1] The molar structural volume changes were calculated by using the value of $\Phi_T = 0.61$.[1,41,47]

TT-LIOAS experiments with solutions of various concentrations of $TSPP^{4-}$ in the presence of various NaCl concentrations yielded a signal which (similar to the case of the monomer[1]) was best-fitted with a biexponential function, affording the values of ΔV_r for triplet formation and decay of different TSPP-monomer−dimer-mixtures. The LIOAS signals for $TSPP^{4-}$ in 10 mM Tris buffer with 140 mM NaCl at $T_{\beta=0}$ obtained upon preferential dimer excitation (651 nm, i.e., 86% dimer excitation) was much smaller than the one with preferential monomer excitation (633 nm, i.e., 53% monomer excitation). In general, the LIOAS signal decreased upon increasing the oligomers (mostly dimers) concentration (Figure 2).

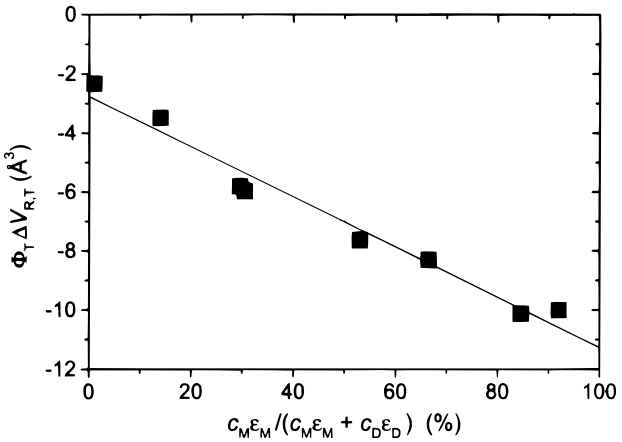

Figure 2. Prompt structural volume change (fast component) of the LIOAS signal after excitation of aqueous solutions of $TSPP^{4-}$ in air-saturated 10 mM Tris as a function of the relative absorption probability of the monomer at the excitation wavelength (λ_{exc}), A_M (%) = (c_M ϵ_M) /(c_M ϵ_M + c_D ϵ_D) × 100 (derived from the absorption spectra, see text). The linear interpolation affords $\Phi_T\Delta V_{R,T} = -11$ Å^3 for the monomer and $\Phi_T\Delta V_{R,T} = -3$ Å^3 for the oligomers, mostly dimers. The conditions of the experiments from right to left were as follows: [A_M (%)/[NaCl] (M)/$TSPP^{4-}$ (μM)/λ_{exc} (nm)] = (92/0/4/355), (85/0/20/532) (66/0.31/2.5/355), (53/0/160/633), (30/0.14/45/532), (30/0.31/22/355), (14/0/160/655), (1/1/20/651).

$\Phi_1\Delta V_{R,1}$ linearly correlated with the monomer $TSPP^{4-}$ absorption probability $A_M = (c_M\epsilon_M)/(c_M\epsilon_M + c_D\epsilon_D)$ (Figure 2) at the excitation wavelength. The value of A_M was calculated by fitting the absorption spectrum at the particular $TSPP^{4-}$ and NaCl concentrations with a weighed sum of the absorption spectra for the pure monomer and for the aggregates (mostly dimers, 430 mM NaCl), under consideration of the molar absorption coefficient of the monomer and the dimer at the excitation wavelength.

The same linear correlation as above was obtained for $\Phi_2\Delta V_{R,2}$ (data not shown). Since Φ_T remains nearly unchanged on going from the monomer to the dimer (20% decrease, Table 1), the decrease in the value of the $\Phi_1\Delta V_{R,1}$ should be attributed to a different structural volume change photoinduced in the dimer.

From a linear extrapolation in Figure 2 and $\Phi_T = 0.61$ (vide supra), the values $\Delta V_{R,1} = -18$ Å^3 for the monomer and $\Delta V_{R,1} = -5$ Å^3 for the dimer were obtained. Similarly, from the decay component values of $\Delta V_{R,2} = 14.5$ Å^3 for the monomer and 4.5 Å^3 for the dimer were obtained.

Zn Complexation of $TSPP^{4-}$. The lifetime of the $ZnTSPP^{2-}$ triplet state after excitation at 568 nm was slightly longer than that of the free base (Table 2). More important, however, were the much smaller values of $\Delta V_{R,1}$ and $\Delta V_{R,2}$ (−3.5 and 3.0 Å^3, respectively) as compared to the values for the free base (Table 2).

TPP in a Micellar Environment. The major difference between TPP and $TSPP^{4-}$ lies in the solubility properties. While TPP is insoluble in water, $TSPP^{4-}$ can be dissolved even up to 100 mM in H_2O. To test whether the interaction of the porphyrin ring with the solvent water molecules has any influence on the structural volume change of the triplet state, LIOAS measurements of TPP incorporated into Triton X-100 micelles were carried out (λ_{exc} = 532 nm). Due to the large excess of the aqueous over the micellar phase, the separation of ΔV_r and ΔV_{th} by a temperature variation was still possible (see Experimental Section). The value of $\Phi_\Delta = 0.58$ for TPP in the micellar system (λ_{exc} = 532 nm) indicates that the triplet yield is high in the

(43) Kruk, N. N.; Dzhagarov, B. M.; Galievsky, V. A.; Chirnovy, V. S.; Turpin, P.-Y. *J. Photochem. Photobiol. B: Biol.* **1998**, *42*, 181.
(44) Reddi, E.; Jori, G. *Rev. Chem. Intermed.* **1988**, *10*, 241.
(45) Krishnamurthy, M.; Sutter, J. R.; Hambright, P. *J. Chem. Soc., Chem. Commun.* **1975**, 13.
(46) Ravikant, M.; Reddy, D.; Chandrashekar, T. K. *J. Chem. Soc., Dalton Trans.* **1991**, 2103 and references therein.
(47) Lambert, C. R.; Reddi, E.; Spikes, J. D.; Rodgers, M. A. J.; Jori, G. *Photochem. Photobiol.* **1986**, *44*, 595.

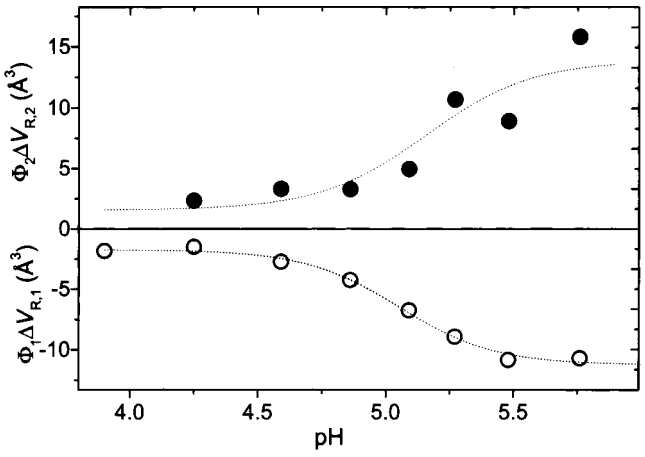

Figure 3. pH dependence of the (○) prompt and (●) slow structural volume changes in a 4 μM $TSPP^{4-}$ air-saturated 100 mM Na acetate solution as determined by the TT method. $\lambda_{exc} = 355$ nm. HCl was used to regulate the pH value. The dotted lines are the result of the fitting using a Henderson−Hasselbalch model, eq 2.

micelle. The contraction in the triplet state, however, decreased strongly to approximately −4 Å^3 with respect to that for $TSPP^{4-}$ (Table 2).

$TSPP^{4-}$ at Various pH Values. In acidic solutions of $TSPP^{4-}$ the structural volume changes accompanying triplet formation and decay were still observable but markedly smaller than in the more alkaline solutions (Figure 3), showing a correlation of the structural volume changes with the proton concentration. The addition of 0.5 M HCl in order to adjust the pH values, only changed the ionic strength from 0.1 to 0.11.

Φ_Δ was essentially unchanged for the acidic form of $TSPP^{4-}$ ($\lambda_{exc} = 355$ nm, Table 1). By assuming $\Phi_T = \Phi_\Delta = 0.51$ (see Table 1), the values $\Delta V_{R,1} = (-5 \pm 1.5)$ Å^3 and $\Delta V_{R,2} = (4 \pm 0.5)$ Å^3 (Table 2) were obtained. The above assumption is justified by the fact that in general, for porphyrins $\Phi_T = \Phi_\Delta$.[36]

$\Delta V_{R,1}$ and $\Delta V_{R,2}$ for $TSPP^{4-}$ in 100 mM acetate solution at various pH values showed a sigmoidal pH dependence, typical of an acid/base equilibrium. Furthermore, the curves for $\Delta V_{R,1}$ and $\Delta V_{R,2}$ are mirror images (Figure 3), that is, the μs expansion has at each pH approximately the same absolute value as the short-lived contraction. The dotted lines in Figure 3 represent fits to the experimental points of a model derived from the Henderson−Hasselbalch eq 2, which describes the pH dependence of an observable a (e.g., absorbance, fluorescence, or ΔV_R in the present case) for the binding of protons to an acceptor molecule.[48]

$$a = a_{min} + (a_{max} - a_{min}) \frac{10^{n(pH-pK_a)}}{1 + 10^{n(pH-pK_a)}} \qquad (2)$$

Here a_{min} and a_{max} are the low and high pH values of the observable a, pK_a has the usual meaning, and n is an empiric parameter (the Hill index) describing the positive ($n > 1$) or negative ($n < 1$) cooperativity of the protonation or deprotonation process. The titration curve obtained with eq 2 has a sigmoidal shape, that becomes steeper for increasing n values. Fitting of the LIOAS data (Figure 3) with eq 2 yielded for the contraction values of $pK_a = 5.1 \pm 0.3$ and $n = 2.3 \pm 0.4$ and for the expansion values of $pK_a = 5.2 \pm 0.3$ and $n = 2.2 \pm 1$ (Table 3), i.e., both values are identical within the experimental error and slightly higher than the reported values for the 2-fold protonation transition (Table 3).

Characterization of the Monoprotonated Species. To understand the factors underlying the pH dependence of $\Delta V_{R,i}$ the pH-induced changes in absorption, the steady state and time-resolved fluorescence in 10 and in 100 mM acetate buffer, and the transient absorbance changes after flash excitation of $TSPP^{4-}$ solutions were analyzed. Figure 4A depicts the absorption spectrum of a 2 μM $TSPP^{4-}$ solution in the 3−6.5 pH range. The resulting pattern is that expected for protonation of the central nitrogens in a porphyrin macrocycle, that is, the Soret band at 413 nm for the basic form shifts to 434 nm in the acidic form.[54] The four bands of basic $TSPP^{4-}$ in the green and red spectral region (Q_y-band, $\lambda_{max} = 633$ nm) are transformed into two bands in the red for the acidic form (Q_y-band, $\lambda_{max} = 645$ nm).

A first inspection of the spectra seems to reveal an isosbestic point at 422 nm. A zoom into the spectral region (Figure 4B), however, clearly shows that the curves do not cross at the same point. The absorption (∼0.03) and wavelength differences (∼2.5 nm) are well beyond the experimental uncertainty. In the Q-band region no isosbestic points were detected either. A third species should thus be present in addition to the free base and the diprotonated forms.

Since a 2-fold protonation of $TSPP^{4-}$ to H_2TSPP^{2-} takes place in the pH range from 6 to 4, the most likely candidate for the third species is the monoprotonated form, that is, $HTSPP^{3-}$. It is unlikely that the third species is an oligomer (e.g., a dimer, vide infra) due to major differences in the spectral and kinetic properties of this species to those known for the dimer. Titration curves of single wavelengths showed in general only one pK_a around 4.8 and a cooperative Hill-index (Figure 4C, Table 3). At certain wavelengths, however, (e.g., 420−425 nm, 550−560 nm) two pK_a's at 5.2−5.5 and 4.4−4.7 (Figure 4D) were found. In these cases a different model function (eq 3) served to simulate the pH-dependent absorption. Now n_1 and n_2 are the Hill indices for the respective transition. The three species in equilibrium have the values a_{min} (species at low pH), a_{med} (species at intermediate pH), and a_{max} (species at high pH) of the observable, e.g., the absorption at a certain wavelength.

$$a = a_{min} + (a_{med} - a_{min}) \frac{10^{n_1(pH-pK_{a,1})}}{1 + 10^{n_1(pH-pK_{a,1})}} + (a_{max} - a_{med}) \frac{10^{n_2(pH-pK_{a,2})}}{1 + 10^{n_2(pH-pK_{a,2})}} \qquad (3)$$

Fitting of the absorption spectra in the Soret band region at the various pH values using a linear combination of the spectra for $TSPP^{4-}$ and H_2TSPP^{2-} afforded bad fits at almost all pHs in the 400−460 nm region (see simulated curve, Figure 5A and residuals distribution, Figure 5B). Good fits were obtained with three Gaussian bands with amplitudes a_j, halfwidths w_j, and central wavelengths xc_j (eq 4). A_{fb} and A_{dp} are the spectra of $TSPP^{4-}$ and of H_2TSPP^{2-}, each determined at extreme pH values (pH 6.5 for $TSPP^{4-}$ and pH 3.0 for H_2TSPP^{2-}), and a_1

(48) Marshall, A. G. *Biophysical Chemistry: Principles, Techniques and Applications*; John Wiley and Sons: New York, Brisbane, Toronto, Chichester, 1978.

(49) Williams, G. N.; Hambright, P. *Inorg. Chem.* **1980**, *19*, 562.
(50) Tabata, M.; Tanaka, M. *J. Chem. Soc., Chem. Commun.* **1985**, 42.
(51) Krishnamurthy, M. *Ind. J. Chem. B* **1977**, *15*, 964.
(52) Shamin, A.; Hambright, P. *Inorg. Chem.* **1980**, *19*, 564.
(53) Turay, J.; Hambright, P. *Inorg. Chim. Acta* **1979**, *35*, L319.
(54) Hambright, P. Dynamic Coordination Chemistry of Metalloporphyrins. In *Porphyrins and Metalloporphyrins*; Smith, K. M., Ed.; Elsevier: Amsterdam, 1975; pp 233−271.

Table 3. Values of the pK_a Values and Cooperativity Hill Index n Obtained for $TSPP^{4-}$ and $TMAPP^{4+}$ with the Techniques as Indicated

compd	technique	pK_a	n	pK_a^3, pK_a^4 lit.[a]
$TSPP^{4-}$	absorption			
	- single λ except 420−425	4.8 ± 0.2[b]	1.5 ± 0.3[b]	4.9[49]
	- single λ 420−425 nm	4.7 ± 0.2, 5.2 ± 0.15[c]	1.2 ± 0.1, 1.4 ± 0.2[c]	4.99,4.76[50]
	- Soret band spectra			
	$TSPP^{4-}$	4.8 ± 0.1[b]	1.7 ± 0.2[b]	
	$HTSPP^{3-}$	4.4 ± 0.1, 5.2 ± 0.2[d]	1.0 ± 0.3, 1.4 ± 0.6[d]	
	H_2TSPP^{2-}	4.6 ± 0.1[b]	1.6 ± 0.1[b]	
$TSPP^{4-}$	fluorescence[e]			
	- single λ except 640−655, 700−705 nm	4.7 ± 0.1[b]	1.9 ± 0.2[b]	
	- single λ 640−655, 700−705 nm	4.5 ± 0.3, 5.5 ± 0.4[c]	1.1 ± 0.1, 1.5 ± 0.2[c]	
	- total emission spectra			
	$TSPP^{4-}$	5.1 ± 0.1[b]	1.8 ± 0.1[b]	
	$HTSPP^{3-}$	4.6 ± 0.1, 5.2 ± 0.2[d]	1.2 ± 0.2, 1.8 ± 0.3[d]	
	H_2TSPP^{2-}	4.9 ± 0.1[b]	1.7 ± 0.2[b]	
	- decay lifetimes			
	τ_1 = 1.3 ns, $HTSPP^{3-}$	4.3 ± 0.3, 4.9 ± 0.3[c]	1.2 ± 0.4, 1.6 ± 0.5[c]	
	τ_2 = 3.4 ns, H_2TSPP^{2-}	4.9 ± 0.1[b]	1.7 ± 0.2[b]	
	τ_3 = 9.6 ns, $TSPP^{4-}$	5.0 ± 0.1[b]	1.5 ± 0.3[b]	
$TSPP^{4-}$	LIOAS[e]			
	$\Delta V_{R,1}$	5.1 ± 0.3[b]	2.3 ± 0.4[b]	
	$\Delta V_{R,2}$	5.2 ± 0.3[b]	2.2 ± 1[b]	
$TMAPP^{4+}$	absorption			
	Soret band spectra			
	$TMAPP^{4+}$	3.8 ± 0.2[b]	1.5 ± 0.2[b]	4.11, 3.95[51]
	$HTMAPP^{5+}$	3.5 ± 0.2, 4.1 ± 0.2[d]	1.5 ± 0.1, 1.7 ± 0.2[d]	3.6[52]
	H_2TMAPP^{6+}	3.5 ± 0.2[b]	1.2 ± 0.3[b]	3.64, 3.62[53]
$TMAPP^{4+}$	fluorescence, total[e]			
	$TMAPP^{4+}$	3.6 ± 0.1[b]	1.4 ± 0.2[b]	
	$HTMAPP^{5+}$	3.4 ± 0.2, 4.0 ± 0.1[d]	1.3 ± 0.3, 1.6 ± 0.2[d]	
	H_2TMAPP^{6+}	3.4 ± 0.2[b]	1.3 ± 0.4[b]	
$TMAPP^{4+}$	LIOAS[e]			
	$\Delta V_{R,1}$	3.5 ± 0.2[b]	1.5 ± 0.2[b]	
	$\Delta V_{R,2}$	4.0 ± 0.2[b]	1.5 ± 0.2[b]	

[a] pK_a^3 refers to the Porph/$PorphH^+$ equilibrium, and pK_a^4 refers to the $PorphH^+$/$PorphH_2^{2+}$ equilibrium. [b] Equation 2. [c] Equation 3. [d] Equations 3 and 4. [e] λ_{exc} = 355 nm.

and a_2 are the relative concentrations at each pH value.

$$A = a_1A_{fb} + a_2A_{dp} + \sum_{j=3}^{5} \frac{\sqrt{2}a_j}{w_j\sqrt{\pi}} \exp(2(\lambda - xc_j)^2/w_j^2) \quad (4)$$

In the pH region with the largest spectral changes (pH 4.4−5.1) the fits were performed with all fit parameters set free. For the monoprotonated species ($HTSPP^{3-}$) very similar positions and halfwidths were obtained with a main maximum at 424.5 nm, a minor maximum at 442 nm and a shoulder at ∼400 nm (vide infra, Figure 8A).

The band positions and halfwidths were then fixed to these average values and the amplitudes were determined for the spectra at the other pH values. Since the integrated absorption cross section of free base ($TSPP^{4-}$) and diprotonated (H_2TSPP^{2-}) forms are almost equal, for the calculation it was assumed that this also holds true for the absorption cross section of $HTSPP^{3-}$. This monoprotonated species shows two pK_a values at 5.2 and 4.4, whereas the other two show only one (Table 3). All derived Hill indices (eq 2) were cooperative. Our pK_a^3 value for the equilibrium $TSPP^{4-}$/$HTSPP^{3-}$ agrees with that reported in the literature (4.9[49] and 4.99[50]), whereas it has been reported that the pK_a^4 value for the equilibrium $HTSPP^{3-}$/ H_2TSPP^{2-} is 4.76.[50]

The above results are in good agreement with the single wavelength analysis but with a much higher precision. The maximum relative concentration of the monoprotonated species $HTSPP^{3-}$ is ∼15% at pH 4.9.

No such detailed evaluation of the spectra could be carried out in the Q-band region due to the lower absorption cross sections and the more complex band structure. To obtain the absorption spectrum of $HTSPP^{3-}$, a similar fitting procedure with the linear combination of A_{fb} and A_{dp} and five Gaussian bands was performed for the spectra at pH 4.8 and 5.0. The most prominent feature is a red-shifted absorption band at 665 nm (see Figure 8B).

The steady-state fluorescence spectra of a 2 μM $TSPP^{4-}$ solution in 100 mM acetate buffer in the pH range 3.5−6.0 (Figure 6A) shows a complex structure of bands, and in particular the presence of two peaks at 645 and 700 nm in the basic form, and the appearance of a peculiar band for the acidic form with maximum at 672 nm.

From the absorbance-normalized, integrated emission (proportional to the fluorescence quantum yield) we conclude that the basic form has a lower Φ_F value than the acidic form. In particular, by using Φ_F = 0.058 ± 0.005 for $TSPP^{4-}$,[1] Φ_F for the simple mixture of free-base and diprotonated forms may be calculated in the whole pH range. For H_2TSPP^{2-} at pH 3.4 and λ_{exc} = 355 nm a value Φ_F = 0.13 ± 0.015 is obtained in accordance with the literature value.[55]

The differences in pK_a values upon titrations of the emission at single wavelengths (Table 3), the absence of isosbestic points, and the bad fits with a linear combination of spectra of only two species indicate that in the fluorescence spectra the contribution of the monoprotonated form should not be neglected either. The addition of two Gaussian bands was sufficient to obtain good fits in the extended linear combination fitting with

(55) Harriman, A.; Richoux, M.-C. *J. Photochem.* **1984**, *27*, 205.

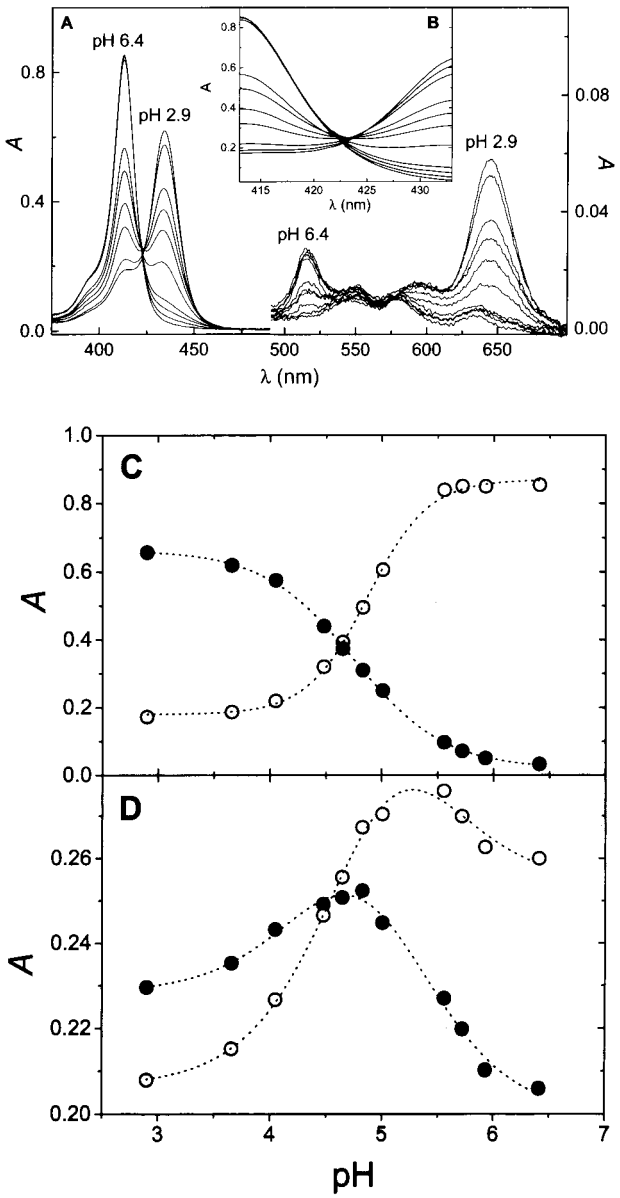

Figure 4. (A) Absorption spectra of a 1.7 μM $TSPP^{4-}$ solution in 10 mM acetate buffer at various pH values in the range 3−6.5. HCl was used for the regulation of the pH value. The Q-band region is enlarged 5 times. (B) Inset: zoom of the absorbance around 422 nm. Absorbance as a function of pH at (C) (○) 413 nm and (●) 433 nm, (D) (○) 422 nm and (●) 423 nm. The dotted lines represent the simulation using eq 2 for C and eq 3 for D. The absorbances refer to the measured values in 4A.

eq 4 (not shown). pK_a's of 5.1 and 5.2 for free base/monoprotonated and of 4.6 and 4.9 (Figure 6B, Table 3) for mono-/diprotonated equilibria and Hill indices >1 give a picture very similar to that derived from the absorption spectra. The resulting emission spectrum of $HTSPP^{3-}$ has a maximum at 684 nm and a faint shoulder at 750 nm (Figure 8C).

The average fluorescence lifetime was longer at high than at low pH values (λ_{obs} = 678 nm). It increased from 3.4 to 9.6 ns (Figure 7) on going from pH 3.95 to 6.16, suggesting that the observed difference in Φ_F arises from the existence of different chemical species at the two extremes. The emission decays were fitted with a sum of single-exponential decay function (Inset in Figure 7). At all pH values at least two decays were needed to fit the data. The lifetimes were almost unaffected by changing the pH. At low pH only the faster decay was detected, whereas at high pH only the slower decay was present. At intermediate

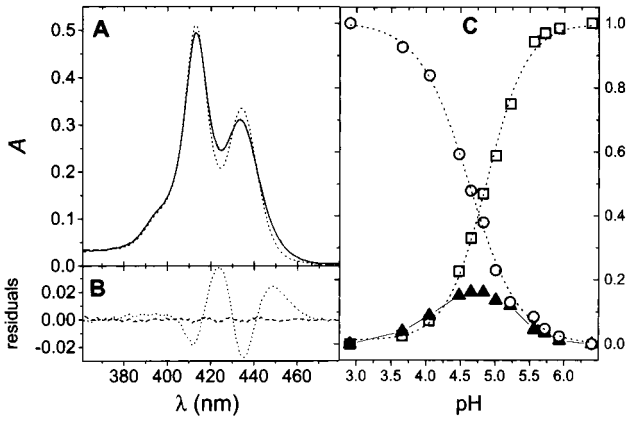

Figure 5. (A) Absorption spectrum of a 1.7 μM $TSPP^{4-}$ solution in 10 mM acetate buffer at pH 4.8 (–) is depicted together with the fit functions by using (···) a sum of two Gaussian functions and (- - -) eq 4. Note that the fitting with eq 4 overlaps the data. The respective residuals are shown in (B). (C) Relative concentration of (□) free base $TSPP,^{4-}$ (▲) monoprotonated $HTSPP^{3-}$, and (○) diprotonated H_2TSPP^{2-} as a function of pH as obtained from the fitting with eq 4. The dashed lines are fits using eqs 2 (□,○) and eq 3 (▲).

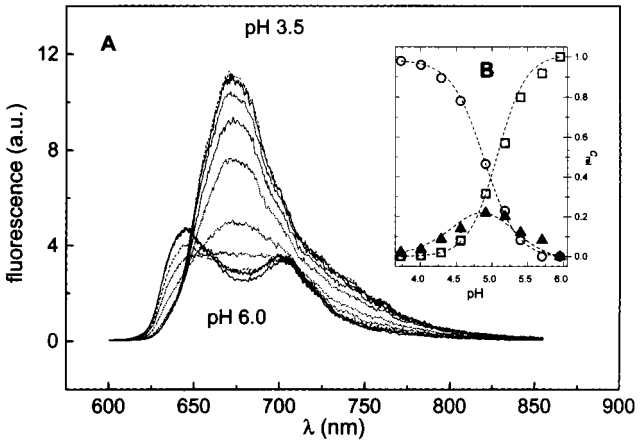

Figure 6. (A) Steady-state fluorescence emission after 355 nm excitation of a 2 μM $TSPP^{4-}$ solution in 100 mM acetate buffer at various pH values in the range 3.5−6.0. (B) Relative concentration of (□) free base, (▲) mono-, and (○) diprotonated forms as a function of pH as obtained from fits using eq 4. The dashed lines represent fits using eqs 2 (□,○) and eq 3 (▲).

pHs 4.5−5.2 a third component was detectable with τ_3 = 1.3 ns and relative amplitude <10%. All of these data agree within experimental error with the data already reported for $TSPP^{4-}$.[56] The short decay component is found in a pH range where the species $HTSPP^{3-}$ appears in the absorption and fluorescence spectra titrations. Thus, this decay component should be assigned to this species rather to an aggregated species as it was speculated.[56]

The fluorescence decays upon 355 nm excitation analyzed with a global procedure using a three-exponential fitting function (τ_1 = 1.3 ns, τ_2 = 3.4 ns, τ_3 = 9.6 ns), afforded three amplitudes a_i which reflect the ionic equilibria of the three species ($TSPP,^{4-}$ $HTSPP^{3-}$, and H_2TSPP^{2-}) similar to the results from absorption and emission spectra. The pK_a's for the free base (5.0) and the diprotonated form (4.9) with Hill indices >1 are essentially the same as the ones from absorption and fluorescence spectra (Table 3). The monoprotonated form has values of pK_a^3 = 4.9 and pK_a^4 = 4.3 with cooperative Hill indices. The disagreement

(56) Schneckenburger, H.; Gschwend, M. H.; Sailer, R.; Rück, A.; Strauβ, W. S. L. *J. Photochem. Photobiol. B: Biol.* **1995**, *27*, 251.

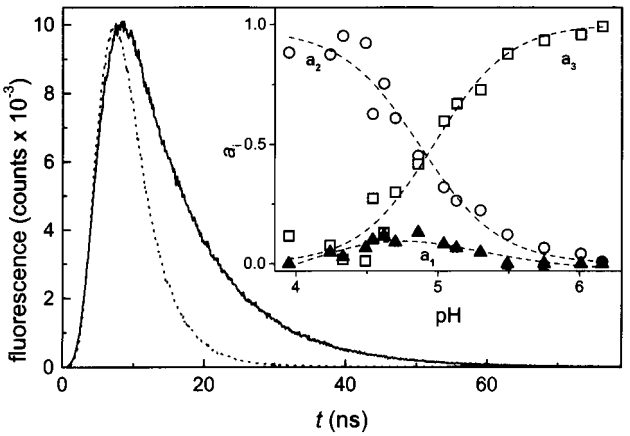

Figure 7. Fluorescence decay signals of a 4 μM solution of $TSPP^{4-}$ in 100 mM acetate buffer at pH 3.95 (lifetime 3.4 ns) and pH 6.16 (lifetime 9.6 ns); $\lambda_{exc} = 355$ nm. Inset: Preexponential factors from a three-exponential global analysis of time-correlated single photon counting signals of a solution of $TSPP^{4-}$ in 100 mM acetate buffer between pH 3.95 and 6.16. (▲) a_1 for $\tau_1 = 1.3$ ns, (○) a_2 for $\tau_2 = 3.4$ ns, and (□) a_3 for $\tau_3 = 9.6$ ns; $\lambda_{exc} = 355$ nm, $\lambda_{em} = 678$ nm. Dashed lines are the result of fits using eqs 2 and 3.

found for pK_a[4] from the titration of τ_1 (4.3) and τ_2 (4.9) should be explained by the relatively large uncertainty in the fluorescence decay analysis with a three exponential decay function.

$TMAPP^{4+}$ at Various pH Values. The pH-dependent properties of $TMAPP^{4+}$ in 0.1 M Na acetate solutions showed a behavior similar to that found with $TSPP^{4-}$, that is, titrations of absorption and fluorescence spectra revealed the existence of a third species in the pH transition region. The protonation occurred at a lower pH (3.5−4.2). In this case, however, the pK_a values derived by titrating the first and the second ΔV_R values are somewhat different. The value $pK_a = 3.5 \pm 0.2$ from the titration of $\Delta V_{R,1}$ (formation of the triplet state), agreed with that related to the equilibrium mono-/diprotonated forms as derived from a fitting of the absorption and emission spectra ($pK_a = 3.5$ and 3.4, Table 3). In this case the reduction of the structural volume change in the triplet state occurred with the formation of the diprotonated H_2TMAPP^{6+} form (Table 3).

On the contrary, titration of $\Delta V_{R,2}$, related to the triplet state decay, showed a $pK_a = 4.0 \pm 0.2$, more similar to pK_a[3] = 4.1 from the absorption and fluorescence data (4.1 and 4.0, Table 3). Two pairs of values have been reported for $TMAPP^{4+}$ pK_a[3]/pK_a[4] = 4.11/3.95[51] and = 3.64/3.62.[53] The values we report are in the same pH region. However, we find a more pronounced splitting between pK_a[3] and pK_a[4]. Clearly, there are great difficulties associated with the determination of these pK_a values by conventional methods. The difference between the pK_a values determined by LIOAS for the triplet state formation and decay is systematic, since in the three sets of experiments the pK_a value for the triplet production was always lower than that for its decay.

Discussion

Nature of the Species at Intermediate pH. Extensive studies on porphyrins have shown that especially the water-soluble derivatives readily undergo cooperative $\pi-\pi$ electrostatic interactions between ionic substituent groups and the electron-rich central nitrogen atoms that result in aggregation. It is known that $TSPP^{4-}$ forms H-type dimers, whereas H_2TSPP^{2-} at high ionic strength forms H- and J-aggregates, the latter comprising more than 20 molecules.[57−59] Although the formation of higher aggregates is unlikely under the conditions used in the present study with relatively low porphyrin concentrations (<20 μM) and low ionic strenght (10 mM unless purposedly larger in order to see the oligomers), the presence of dimers cannot be excluded. The absence of higher aggegates is supported by the large values of Φ_Δ measured.[37] The following calculation shows, however, that in general the dimers concentration is very low under our conditions. The literature values for the dimerization constant of $TSPP^{4-}$, K_D, are very disperse (near 0 at ionic strengths 0−0.1,[60] 21 000 M^{-1} at ionic strength 0.11,[61] and 96 000 M^{-1} at ionic strength 0.06[62]), and there are no reports for the K_D value of H_2TSPP^{2-}. We estimated a value of $K_D = 10\,000$ M^{-1} in 10 mM Tris and acetate buffers and <30 000 M^{-1} in 100 mM acetate buffer for $TSPP^{4-}$ and H_2TSPP^{2-}. Considering that the porphyrin concentration was ~1.6 μM in the absorption titration experiments, it is calculated that the dimer concentration is <1.5%.

To rule out the dimer influence, experiments were repeated in 100 mM acetate buffer in which a dimer concentration of ~4.5% is calculated (by using $K_D = 96\,000$[62] the dimer concentration would be 16%). The titrations as well as the spectrum derived for the intermediate species, assigned to $HTSPP^{3-}$ (data not shown) are nearly identical to those found in 10 mM acetate buffer. This led us to conclude that dimer formation has no influence on the titrations of absorption spectra. The same holds for the titrations of the fluorescence properties performed only in 100 mM acetate buffer at 2−4 μM $TSPP^{4-}$ (vide supra). The values of the structural volume changes, however, might be lower due to the presence of a larger percentage of oligomers (mostly dimers) at the higher concentrations used in the LIOAS experiments (Figure 2). This, however, does not invalidate our conclusions about the factors determining the structural volume changes (see next section). Thus, both at 100 and 10 mM buffer, absorption and fluorescence spectra in the intermediate pH range are assigned to the monoprotonated porphyrin with spectral features shown in Figure 8, different from those reported for $(TSPP^{4-})_2$.

For $TMAPP^{4+}$ the third species should also be attributed to the monoprotonated $HTMAPP^{5+}$, based on the evaluation made with the reported value of $K_D = 10^3$ M^{-1} in water which affords a concentration of dimer of ~2% under the conditions of the present studies.[51]

Origin of the Structural Volume Changes. As already stated in our previous publication on $TSPP^{4-}$, the prompt component of the LIOAS signal includes all relaxation processes up to triplet formation.[1] Thus, although the prompt contraction observed for each of the porphyrins can be attributed to the triplet formation, we cannot exclude that it already takes place upon formation of the excited singlet state.

We speculated about the possible origin of the contraction concomitant with the triplet state formation after excitation of $TSPP^{4-}$.[1] Support for the idea of a larger electron density at the nitrogen atoms of the porphyrin in the ground state was found in results of resonance Raman studies and semiempirical

(57) Ribó, J. M.; Crusats, J.; Farrera, J.-A.; Valero, M. L. *J. Chem. Soc., Chem. Comm.* **1994**, 681.
(58) Maiti, N.; Ravikanth, M.; Mazumdar, S.; Periasamy, N. *J. Phys. Chem.* **1995**, *99*, 17192.
(59) Akins, D. L.; Özçelik, S.; Zhu, H.-R.; Guo, C. *J. Phys. Chem.* **1996**, *100*, 14390.
(60) Fleischer, E. B.; Palmer, J. M.; Srivastava, T. S.; Chaterjee, A. *J. Am. Chem. Soc.* **1971**, *93*, 3162.
(61) Sutter, T. P. G.; Rahimi, R.; Hambright, P.; Bommer, J. C.; Kumar, M.; Neta, P. *J. Chem. Soc., Faraday Trans.* **1993**, *89*, 495.
(62) Krishnamurthy, M.; Sutter, J. R.; Hambright, P. *J. Chem. Soc., Chem. Commun.* **1975**, 13.

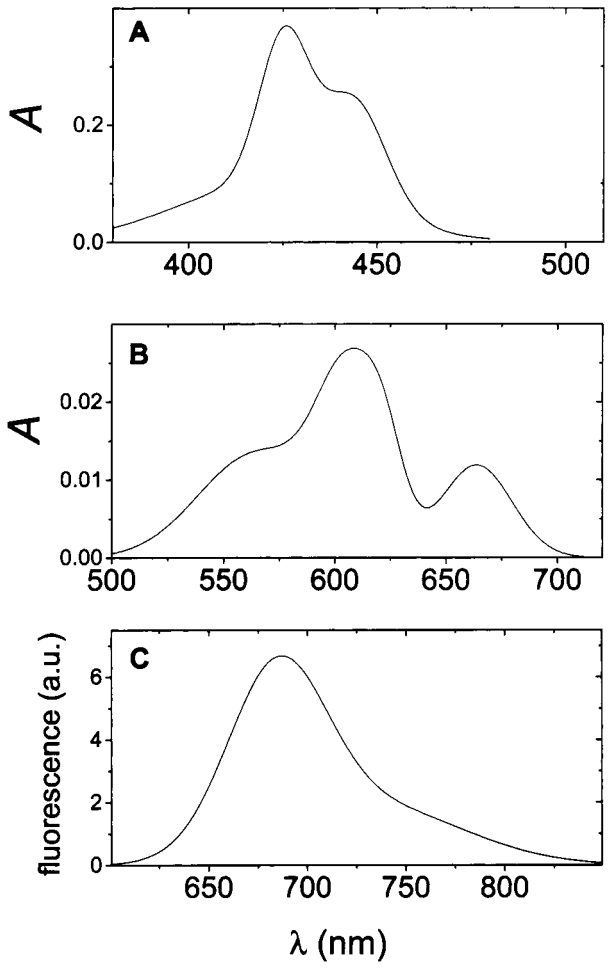

Figure 8. Absorption spectrum of the monoprotonated species $HTSPP^{3-}$ in the (A) Soret band region, and (B) Q-band region; (C) fluorescence spectrum of $HTSPP^{3-}$. All spectra obtained from fits at different pH values using eq 4.

calculations.[63,64] We suggested that the contraction determined upon excitation is due to the fact that the four nitrogen atoms in the macrocycle are stronger hydrogen-bonded with the surrounding water molecules in the excited state than in the ground state.

In the present study we varied the porphyrin system itself in a number of ways and changed the porphyrin environment.

The character of the meso substituents is, if at all, only slightly involved in the generation of the structural volume change, as revealed by the similarity in the contraction in the range 16−18 Å3 upon triplet formation of the free base forms for the three meso-substituted porphyrins containing either negatively ($TSPP^{4-}$) or positively ($TMPyP^{4+}$ and $TMAPP^{4+}$) charged groups (Table 2). Thus, the large values of the contraction seem to be inherent to the free base form of the porphyrin ring.

Inasmuch as the triplet yield was nearly constant for all systems as verified by TRPD and LFP ($\Phi_T \geq 0.5$, Table 1), we can exclude that the observed decrease of the structural volume change in the diprotonated forms H_2TSPP^{2-} and H_2TMPP^{6+} or in the dimer $(TSPP^{4-})_2$ arises from a decrease in the yield of formation of the triplet state.

In the oligomers (mostly dimers under our conditions) the partial overlap of the two porphyrin macrocycles obviously[45] shields the nitrogen atoms, leading to a lower contraction in the triplet state (Table 2). A similar small contraction is obtained for $ZnTSPP^{2-}$ (Table 2). Also in this case we attribute the smaller value of ΔV_R to a lower hydrogen-bonding capability as compared to the free base. Preliminary semiempirical calculations performed by M. Zerner (University of Florida) on gas-phase Mg-porphyrin indicate that the electron density on the nitrogens is effectively slightly larger in the excited states than in the ground states, and more so in the triplet states (M. Zerner, private communication).

The 5-fold reduction in the value of $\Delta V_{R,1}$ found for TPP incorporated in the micelles (Table 2) can be also explained by the blocking of the interactions with water of the lone pairs on the porphyrin nitrogen atoms.

At pH 3.5, where the tetrakis(4-sulfonatophenyl) porphyrin is mainly diprotonated, the contraction of the triplet state was lowered by a factor of 4 relative to that of the free base $TSPP^{4-}$ (Table 2), while the triplet yield remained the same (Table 1). In this case the proton is already attached to the nitrogen in the ground state and the volume difference between triplet and ground state is much smaller. The same conclusions apply to $TMAPP^{4+}$ (from a contraction of 16 $Å^3$ at pH 7 to 4 $Å^3$ at pH 3, Table 2).

The reduction of $\Delta V_{R,i}$ can be thus effected by various mechanisms all implying the blocking of the interaction of the N atoms with water. In the case of dimerization and metal complexation the porphyrin nitrogen atoms are simply not available for interactions with the surrounding water molecules. For the case of porphyrin embedded into a micelle there is a hydrophobic barrier impairing the contact between the nitrogen atoms and the water molecules. In the diprotonated porphyrin at pH < 3.5 the ground state interacts already strongly with the two protons bound to the porphyrin.

Thus, the contraction in the triplet state of $TSPP^{4-}$ and of $TMAPP^{4+}$ is indeed to a large extent (−12 $Å^3$) due to a larger specific interaction in the triplet state of the center of the porphyrin macrocycle with water, whereas a smaller contribution of ∼−4 $Å^3$ to the total contraction should originate in shortening of bonds in the macrocycle in the triplet state. This latter amount is the value of the contraction $\Delta V_{R,1}$ for triplet formation (and the expansion $\Delta V_{R,2}$ for its decay) of the acidic forms, of the dimeric form at neutral pH, and of $ZnTSPP^{2-}$.

The pH dependences of $\Delta V_{R,1}$ and $\Delta V_{R,2}$ should be related to those of the absorption and fluorescence properties. For $TSPP^{4-}$ the pK_a's of the structural volume change is higher (5.2) than that from absorption and fluorescence data without consideration of the monoprotonated species (4.85, Table 3). By including the monoprotonated forms $HTSPP^{3-}$ and $HTMAPP^{5+}$, the pH dependence of the absorption and emission spectra of these porphyrins served to explain the pK_a values derived from the titrations of the structural volume changes.

In the case of $TSPP^{4-}$, the larger pK_a value of 5.2 found upon titration of the structural volume change for the formation and for the decay of the triplet state correspond to pK_a[3] for the free-base/monoprotonated equilibrium as determined from the fitting of the absorption and emission spectra upon consideration of three species (Table 3), that is, the structural change takes place upon monoprotonation.

In the case of $TMAPP^{4+}$, however, the pK_a = 3.5, derived from the titration of $\Delta V_{R,1}$ coincides with pK_a[4], that is, the contraction upon triplet formation is concomitant with the mono/diprotonated equilibrium, whereas the expansion upon triplet decay (pK_a = 4) is related to the monoprotonated/free base equilibrium (Table 3).

(63) Bell, S. E. J.; Aakeröy, C. B.; Al-Obaidi, A. H. R.; Hegarty, J. N. M.; McGarvey, J. J.; Lefley, C. R.; Moore, J. N.; Hester, R. E. *J. Chem. Soc., Faraday Trans.* **1995**, *91*, 411.

(64) Bell, S. E. J.; Al-Obaidi, A. H. R.; Hegarty, J. N. M.; Hester, R. E.; McGarvey, J. J. *J. Phys. Chem.* **1993**, *97*, 11599.

At the moment we have no straightforward argument to explain why the pK_a derived from the titration of the $\Delta V_{R,1}$ should correspond to different equilibria for $TSPP^{4-}$ and $TMAPP^{4+}$. In fact, the titration of $\Delta V_{R,2}$ corresponds in both cases to the monoprotonated/free base equilibrium. Perhaps small differences in the excited states pK_a values for the ground and excited states are responsible for the differences. The already difficult fitting of the spectra impair a proper evaluation of the pK_a* values.

The small contraction of $\sim$4 Å^3 determined for the fully protonated forms of both porphyrins titrated, the dimer and the Zn complex of $TSPP^{4-}$, is similar to that recently reported for the triplet formation in uroporphyrin.[21] On the basis of our data we suggest that in these very crowded macrocycles the small contraction associated with the formation of the triplet state is essentially due to bond length changes without a contribution of the solvent shell, in contrast to the suggestion by the authors that a change in bonding to ligated H_2O molecules is responsible for the contraction.

Acknowledgment. C.V. acknowledges an EC-HCM Grant No. ERBCHBGCT930313. We thank Ethel Hüttel, Sigrit Russell, Peter Schmidt, and Andrea Keil-Block for their able technical assistance. We are indebted to Professor Kurt Schaffner for his steady support of and interest in this project and to Professor Mike Zerner (University of Florida, U.S.A.) for the INDO calculations on Mg-porphyrin.

JA9913885